High adsorption of fulvic acid by amino modified styrene-type macroporous resin and evaluation of its mechanism

Munan Zhao and Chongwei Cui

ABSTRACT

Amino-modified HPD 100 styrene-type macroporous resin (M-HPD 100) was successfully synthesized by the atom transfer radical polymerization process. The modified resin showed excellent performance in the degradation of fulvic acid (FA). FA removal was pH, temperature and flow velocity dependent. The adsorption data could be well interpreted by the Freundlich model. The maximum adsorption efficiency for M-HPD 100 obtained from the Freundlich model was 92.5% at 298 K, which was 37% higher than that of unmodified styrene-type macroporous resin (HPD 100). The adsorption process could be described by the pseudo-second-order kinetic model. The intra-particle diffusion and film diffusion were believed to be the rate-limiting process for both adsorbents. Thermodynamic parameters suggested it was a multi-layer physicochemical process. More importantly, although limited improvements were seen, the results of this study suggested that the surface of resin can be modified with functional groups to enhance the adsorption of FA from aqueous solution and may give other advantages; for example, despite the interference of the pore diffusion coefficient and other substances, M-HPD 100 has excellent regeneration capacity, and the adsorption and desorption efficiency was 74% and 64.28% respectively after six regenerations, which proved it has engineering application value.

Key words | adsorption, characterization, fulvic acid, M-HPD 100, regeneration

Munan Zhao
Chongwei Cui (corresponding author)
State Key Laboratory of Urban Water Resource and Environment,
Harbin Institute of Technology,
Harbin 150090,
China
E-mail: *18845181188@126.com*

HIGHLIGHTS

- M-HPD 100 shows excellent performance in the degradation of fulvic acid.
- Adsorption process for M-HPD 100 includes not only physisorption but also chemisorption.
- Intra-particle diffusion and film diffusion are believed to be the rate-limiting processes for M-HPD 100.
- M-HPD 100 has good regeneration capacity after six regenerations.

INTRODUCTION

Due to the specific climate and natural geological conditions in northeast China, the raw water is rich in humic substances, and the conventional water purification process (coagulation–precipitation–filtration–disinfection) has limited ability to remove natural organic matter (NOM), which is an important precursor to lead to disinfection by-products (Matilainen & Sillanpää 2010). There are various kinds of methods for NOM removal such as filtration (Ang *et al.* 2015), chemical precipitation (Sillanpää *et al.* 2018), adsorption (Sophia & Lima 2018) and ion exchange process (Bolto *et al.* 2002). Among these methods, adsorption is one of the most economically favorable and technically easy methods (Bhatnagar & Sillanpaa 2017).

Styrene-type macroporous adsorbent resin has experienced rapid growth due to its remarkable advantages such as diverse synthesis methods, easy functionalization, high surface area, low cost reagents and mild operating conditions (Tan & Tan 2017). These polymers can be readily modified

doi: 10.2166/wst.2020.187

to tailor physical and chemical properties and improve selectivity by reducing competitive adsorption in environments containing mixed pollutants (Zhu *et al.* 2011). Styrene-type macroporous resin is a kind of nonpolar copolymer, which takes styrene with small dipole moment as a polymerization monomer (Cheng *et al.* 2018). Fulvic acid (FA), as a reversible hydrophilic colloid with negative charge, has a complex and unfixed structure in water, and is composed of alkyl aromatic hydrocarbon units, such as the carbonyl group, carboxyl group, phenolic hydroxyl group and other active groups (Aeschbacher *et al.* 2012). Few studies have been done on the adsorption properties of FA after graft modification of styrene-type macroporous resin.

The amino group grafted onto the resin's surface as an alkaline group can change the surface electrification and polarity of resin, and thus affect its adsorption behavior. Wu *et al.* (2019) reported that slight changes have been found in the pore diameter of resin after surface modification, which ensured the suitability of the modified resin aperture to the FA's particle size. It was speculated that by increasing the specific surface area of styrene-type macroporous adsorbent resin after graft modification (Zheng 2011), the surface properties of the resin may be further enhanced to have a better adsorption performance on FA, which has a specific molecular weight level in water.

In this paper, amino-modified HPD 100 styrene-type macroporous resin (M-HPD 100) was prepared by atom transfer radical polymerization (ATRP) (Matyjaszewski 2012). In fixed-bed column systems, the effects of the process parameters such as pH, temperature, and flow velocity on FA removal were investigated. To better understand the adsorption characteristics, some isotherm, kinetic and thermodynamic models were employed to evaluate the sorption process. Furthermore, raw water samples were used to research the improvement of FA adsorption selectivity by reducing competitive adsorption in environments containing mixed pollutants. The FA adsorption capacity and kinetics of unmodified styrene-type macroporous resin (HPD 100) and M-HPD 100 were studied, in addition to improving adsorption performance; therefore, this study provides insight into optimum regeneration conditions for polymers saturated with sodium hydroxide (NaOH).

MATERIALS AND METHODS

Materials

All the selected chemicals were analytical grade reagents. Methyl chloride ether (CME), zinc chloride ($ZnCl_2$), methyl alcohol (MA) and trimethylamine (TMA) were purchased from China Pharmaceutical (group) Shanghai Chemical Reagent Co. Ltd (Shanghai, China). HPD 100 and HPD 300 were purchased from Cangzhou Bon Adsorber Technology Co., Ltd (Hebei, China). D 101 was obtained from Anhui San Xing Resin Technology Co., Ltd (Anhui, China). Toluene was obtained from Tianjin Kemio Chemical Reagent Co. Ltd (Tianjin, China). FA was obtained from Shenyang Jin Nuo Chemical Co. Ltd (Liaoning, China). The laboratory water was double distilled water.

Methods

Fourier transform infrared transmission spectroscopy was undertaken on a Bruker IFS 66 V/S spectrometer (KBr pellet) in the region 4,000–400 cm^{-1}. Elementary analysis was performed by VarioEL (Germany). Thermogravimetric analysis was determined by a thermal analysis instrument (PerkinElmer, PyrisDiamond) in air at a heating rate of 10 $^{\circ}C\ min^{-1}$. The specific surface area, pore size and pore volume of resin was obtained by using the Brunauer–Emmett–Teller (BET) adsorption method (Micromeritics Instrument Corporation, TRI-STAR3020, USA). Adsorbent morphology was examined by scanning electron microscopy (SEM) (Carl Zeiss, EVOMA10, Germany) at magnifications of 500 and 3,000.

Synthesis of M-HPD 100

The synthesis route was similar to what we reported previously (Matyjaszewski 2012). Two grams of pretreatment macroporous resin (Deng *et al.* 2004) and 60 mL of CME were added to 250 mL four-neck bottles, equipped with thermometer and stirrer, then stirred for 2 h at 301 K. Sixteen grams of $ZnCl_2$ was added every half an hour, three times in total, and when the temperature in the four-neck bottles was stable, the temperature was raised to 318 K, and then 16 hours of chloromethylation occurred in the reactor. The resin was filtered and washed with ethanol and deionized water; then it was dried in a vacuum dryer to obtain chloromethylated macroporous resin.

The chloromethylated macroporous resin was washed with MA for an hour and rinsed with deionized water until the pH of the effluent was 7. NaOH was added to adjust the pH value to be greater than 12; once this pH value remained stable for half an hour, the system was washed with plenty of deionized water until the system was between pH 7 and 8. Then the macroporous adsorption resin modified by grafting with amino group was prepared

by quickly adding 30 ml TMA and 2 ml NaOH, leaving to stabilize for the first half an hour and then stirring for another 6 h at 318 K. Finally the macroporous adsorption resin modified by grafting with amino group was prepared after filtration.

Sorption experiments

The sorption kinetics experiments were carried out by shaking 2 g of resin and 400 mL of 10 mg/L FA solution at neutral pH for different time intervals. The adsorption isotherm experiments were determined by mixing 2 g of resin and 400 mL of FA solution with desired concentrations (5–30 mg/L) and shaking for 4 h. The device for the dynamic adsorption experiment was a custom-made glass adsorption column with a jacket (Φ 20 × 150 mm); a schematic diagram of the dynamic adsorption device is shown in Figure S1 (Supplementary Material). The configured FA solution was pumped by a peristaltic pump from top to bottom into the adsorption glass column and the flow rate was adjusted to 4–12 BV/h (BV: bed volume). An automatic fraction collector was programmed according to the requirements to sample at specific time intervals and a total organic carbon (TOC) tester was used to analyze the concentration of effluent FA solution until the adsorption penetration point was reached; then the penetration curve was drawn. Fixed-bed column tests were carried on the effect of pH, temperature and flow velocity on FA removal by adding 2 g of M-HPD 100 and adding 10 mg/L FA solution consistently. The effect of pH on FA removal at temperature 298 K, flow velocity 4 BV/h, was studied by adding 2 g of M-HPD 100 and 10 mg/L of FA solution at pH 6–8 for 1 h. To adjust the pH, 1 mol/L HCl and 1 mol/L NaOH were used. The effect of temperature on FA removal at pH 7, flow velocity 4 BV/h, was studied by adding 2 g of M-HPD 100 and 10 mg/L of FA solution for 1 h at 288–313 K. The effect of flow velocity on FA removal at pH 7, temperature 298 K, was carried out by adding 2 g of M-HPD 100 and 400 mL of 10 mg/L FA solution at 4–12 BV/h. The amount of adsorbed FA was calculated by a mass balance between the initial and equilibrium concentrations.

After determination of concentration of FA versus time, the FA removal percentage (R %) was calculated by Equation (1) (Ghaedi *et al.* 2014):

$$\mathrm{R}\,\% = \left(\frac{C_0 - C_t}{C_0}\right) \times 100 \tag{1}$$

The concentration of FA on the adsorbent surface at equilibrium was calculated by Equation (2) (Hasan & Jhung 2015):

$$q_e = \frac{(C_0 - C_t) \times V}{m} \tag{2}$$

where q_e is the adsorption capacity in mg/g, C_0 and C_e are the initial and equilibrium concentrations of FA in mg/L, V is the volume of FA solution in mL, and m is the mass of adsorbent used in mg.

Desorption experiments

The loaded resin was separated by filtration and rinsed with a small quantity of deionized water. The FA-loaded resin was dried in air for 1 day. Then, 0.2 g of loaded resin was mixed with 30 mL of NaOH solution and shaken for 60 min. The adsorption amount of regenerated resin on FA was also evaluated. After regeneration with 50% NaOH solution, the resin was washed with deionized water and dried at 60 °C. Then, 0.2 g of regenerated resin was shaken with 400 mL of 10 mg/L FA solution at initial pH 7.0 for 60 min.

Mathematical models

The pseudo-first-order model (Equation (3)) (Eris & Bashiri 2016) and pseudo-second-order model (Equation (4)) (Ho & McKay 1998) are expressed respectively, as:

$$\ln(q_e - q) = \ln q_e - \frac{t}{2.303} k_1 \tag{3}$$

$$\frac{t}{q_t} = \frac{1}{k_2 q_e^2} + \frac{t}{q_e} \tag{4}$$

where q and q_e are the amount of FA adsorbed at time t and at equilibrium, respectively, k_1 (min^{-1}) is the rate constant of pseudo-first-order model adsorption, and k_2 ($\mathrm{g\,min^{-1}\,mg^{-1}}$) is the rate constant of pseudo-second-order model adsorption.

The intra-particle diffusion model can be described as follows (Hu *et al.* 2011):

$$q = k_p * t^{\frac{1}{2}} + C \tag{5}$$

where k_p is the intra-particle diffusion rate constant ($\mathrm{mg\,g^{-1}\,min^{-0.5}}$) and C is the adsorption constant and the graph intercept.

Langmuir (Zhang & Wang 2010) and Freundlich (Lin *et al.* 2012) adsorption isotherms can be represented respectively as:

$$\frac{C_e}{Q_e} = \frac{1}{q_m K_L} + \frac{C_e}{q_m} \tag{6}$$

$$Q_e = K_f \cdot C_e^{\frac{1}{n}} \tag{7}$$

where Q_e and C_e are adsorbed value (mg/g) of FA and concentration (mg/L) of FA at equilibrium, respectively. K_L is the Langmuir constant (L/mg) and K_f is the Freundlich constant ($mg^{1-n}\,L^n\,g^{-1}$). q_m is the maximum adsorption capacity (mg/g) of the adsorbent, and n is the degree of dependence of sorption capacity with equilibrium concentration.

The Gibbs free energy change of the sorption reaction is given by the following (Fan *et al.* 2008):

$$\Delta G = -RT \ln K_e \tag{8}$$

$$\Delta G = \Delta H - T\Delta S \tag{9}$$

where K_e is the equilibrium constant, which can be obtained from Freundlich isotherms at different temperature, R is the universal gas constant, 8.314 J/(mol·K), and T is absolute temperature (K). ΔH and ΔS are enthalpy change and entropy change, respectively, and were obtained from the slope and intercept of the plot of Gibbs free energy change vs. temperature.

RESULTS AND DISCUSSION

Adsorbate and adsorbent characterization

The water of Mopanshan Reservoir was filtered by a 0.45 μm membrane and the filtered water was classified by molecular weight in the Minitan TM ultrafiltration system. Detailed steps of hierarchical experiments have been described before (Cabaniss *et al.* 2000). Using three-dimensional fluorescence spectrum analysis, it was determined that the natural organic compounds in the water of Mopanshan Reservoir were mainly humic acid and FA macromolecules, but mainly FA, with the main molecular weight distribution range of 5,000–10,000 Da, accounting for 34%.

Figures S2 and S3 (Supplementary Material) show infrared spectra of HPD 100 and M-HPD 100. In addition to the characteristic absorption peak of polystyrene in Figure S2, 3,470.5 cm^{-1}, 3,368.6 cm^{-1} and 744.8 cm^{-1} in Figure S3 represent the symmetric stretching vibration, anti-symmetric stretching vibration, and internal and external bending stretching vibration of -CH_2NH_2 respectively, which indicated that the amine group was successfully grafted into HPD 100 (Jiang *et al.* 2007; Zhang *et al.* 2009; Xiao *et al.* 2016). In Figure S4, the appearance of amino-modified styrene-type macroporous resin before and after reaction was observed by SEM; after 3 hours of reaction, the nanoscale pores between the gel particles were significantly reduced, indicating that the surface thickness of the material was enhanced by the polymer brush, which may lead to higher adsorption properties of M-HPD 100 for FA (Zhang *et al.* 2009).

Table 1 shows physical properties of four styrene-type macroporous resins (HPD 100, HPD 300, D-101, M-HPD 100); for HPD 100, HPD 300 and D 101, Cangzhou Bon Adsorber Technology and Anhui San Xing Resin Technology have provided the BET surface area and average pore diameter (Table 1). The results reported herein for HPD 100, HPD 300, and D-101 are close to these values. M-HPD 100 has a significant increase (49.23%) in BET surface area and a slight decrease (2%) in mercury porosity when compared to HPD 100, which is consistent with what Zheng (2011) and Tang *et al.* (2009) have reported before. The surface morphology analysis by SEM and transmission electron microscopy for the changes of resin matrix material grafted with amino groups were determined to be similar to the results previously reported (Cheng *et al.* 2018; Wang *et al.* 2019). The surface area of M-HPD 100 was remarkably increased by the polymer brush; it was speculated that amino adhered to the surface pore sites of HPD 100, thus reducing porosity and total pore volume, while the polymer brush increased surface area (Zheng 2011).

Studies have concluded that the interaction between adsorbent and adsorbate was mostly driven by five different forces in the order of sieving effect > electrostatic interactions > hydrophobic interaction (hydrophobic amino

Table 1 | Pore structure parameters of resin matrix material and the graft product

Parameter	HPD 100	HPD 300	D-101	M-HPD 100
BET surface area (m^2/g)	650 650–700	800 800–870	550 500–550	970
Average pore diameter (Å)	85 80–90	98 90–100	54 50–55	83
Average grain diameter (mm)	0.5	0.5	0.5	0.5

Data source: www.bonchem.com/eng/products3.asp, https://sxsz.lookchem.com/.

acids >25%) > hydrogen bonds > π-π stacking interaction (Wang *et al.* 2019), and the average pore diameter, specific surface area and surface electrification of resin were the main factors to determine its adsorption efficiency. Also, the adsorption efficiency is the highest only when the ratio of pore diameter and adsorbent size is 6:1 (Liu *et al.* 2003). Therefore, although HPD 100 does not have the maximum specific surface area, its pore size is more conducive to adsorption of the specific molecular weight of FA in natural water, so HPD 100 can be used as a further research object, and M-HPD 100 will have a better adsorption performance due to its large surface area, specific pore size and surface chemistry.

Kinetics studies

Batch experiments were conducted to explore the rate of FA adsorption onto HPD 100, HPD 300 and D 101. In both systems, Figure S5 and Figure 1(a) show that adsorption quantity of FA increased quickly in the first 10 min and achieved adsorption equilibrium within 45 min. It was noted that the adsorption efficiency of FA on HPD 100, HPD 300, D 101, and M-HPD 100 was 73.6%, 65.45%, 57.43%, and 92.5%, respectively; thus, M-HPD 100 was selected as the best adsorbent for its proper physical properties and adsorption performance.

Processing of kinetic adsorption data can be conducted to understand adsorption dynamics in terms of the order of the rate constant. According to Equations (3) and (4), the calculated regression coefficients for the kinetic models for HPD 100 and M-HPD 100 are documented in Table 2. Figure 1(a) and 1(b) show the plots of the pseudo-first-order model and the pseudo-second-order model, respectively. It was found that the sorption kinetics of HPD100 and M-HPD100 on FA can be better fitted by the pseudo-second-order kinetic model ($R^2 = 0.9902$ and 0.9936, respectively). Thus, experiment results support the assumption behind the model that the rate-limiting step in adsorption of FA is chemisorption involving sharing or exchanging of electrons between adsorbate and adsorbent. It was concluded that the FA adsorption capacity of M-HPD 100 was 1.37 times more than that of HPD100. The increase in the adsorption capacity for FA was mainly attributed to the changes of surface area, surface structure and chemical composition of HPD 100 (Cheng *et al.* 2018).

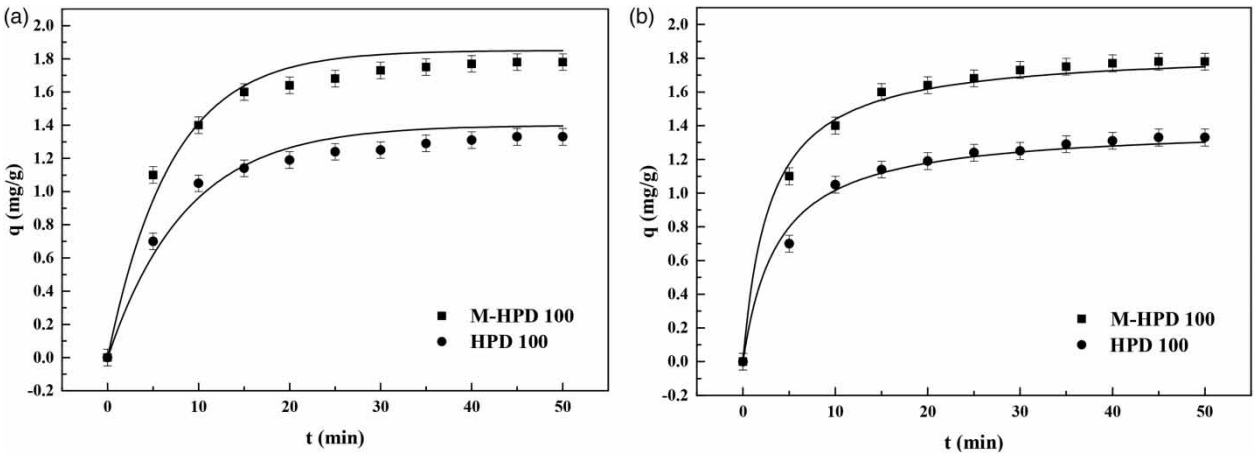

Figure 1 | The adsorption kinetics of FA on HPD 100 and M-HPD 100. The lines are the curve fitting using pseudo-first-order kinetic model (a) and pseudo-second-order kinetic model. (b) Pretreated macroporous resins of 2 g each, $C_0 = 10$ mg/L, $V_0 = 400$ mL, T = 298 K, pH = 7, constant temperature water bath with oscillator speed 130 rpm.

Table 2 | The calculated parameters of the pseudo-first-order and pseudo-second-order kinetic models

	Pseudo-first-order			Pseudo-second-order		
Samples	**Fitted equation**	**R^2**	**K_1**	**Fitted equation**	**R^2**	**K_2**
HPD 100	$\ln(1.4-q) = -0.1164t + 0.3365$	0.9625	0.268	$t/q = 2.6853t + 4.1086$	0.9902	0.190
M-HPD 100	$\ln(1.85-q) = -0.1442t + 0.6152$	0.9712	0.332	$t/q = 0.5405t + 1.5544$	0.9936	0.189

Intra-particle diffusion studies

The adsorption process on a porous adsorbent will generally have a multi-step process. To investigate the mechanism of the adsorption of FA onto HPD 100 and M-HPD 100, the experimental data were tested against the intra-particle diffusion model to identify the mechanism involved in the sorption process. The three consecutive steps in the sorption of FA by a porous sorbent are: (i) mass transfer across the external boundary layer film of liquid surrounding the outside of the particle; (ii) adsorption at a site on the surface (internal or external), the energy of which will depend on the binding process (physical or chemical); this step is often assumed to be extremely rapid; (iii) diffusion of the adsorbate molecules to an adsorption site either by a pore diffusion process through the liquid-filled pores or by a solid surface diffusion mechanism (Cheung *et al.* 2007).

From the intra-particle diffusion model (Equation (5)), the adsorption of FA by a typical size of pores can be observed. A plot of FA adsorbed versus the square root of time (q vs. $t^{1/2}$) presented a multi-linearity correlation, as seen in Figure 2, indicating that two or more steps occurred during the adsorption process (Lalley *et al.* 2016). The first phase (i.e. the steeper portion) represented external mass transfer or film diffusion. The values of C (as seen in Table 3) were not equal to 0; thus, it was postulated that a combination of intra-particle diffusion and film diffusion were rate-limiting phases. The second phase was the equilibrium stage where intra-particle diffusion began to slow because: (a) the pores for diffusion became smaller; (b) the electrostatic repulsion of the adsorbent surface was enhanced; (c) the solute concentration in solution became very low.

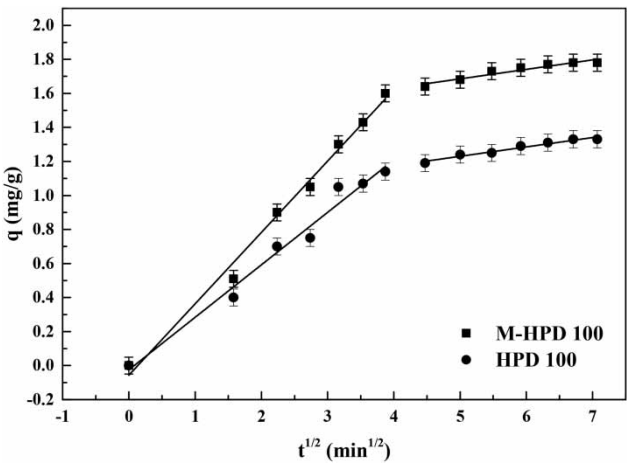

Figure 2 | Intra-particle diffusion kinetics for FA adsorption onto HPD 100 and M-HPD 100.

It was surmised that HPD 100 and M-HPD 100 rapidly adsorbed FA onto its external surface, and then FA was slowly transported by intra-particle diffusion into the particle and retained in the pores. The intra-particle rate constant k_p and C were calculated from the plot in Figure 2 and the results are reported in Table 3.

While the lines for the plot of q_t vs. $t^{1/2}$ are near the origin, due to the double nature of intra-particle diffusion (both film and pore diffusion) (Figure 2), further data analysis can provide more insight into the rate-controlling step. Figure S6 was used to determine the actual rate controlling step involved in the sorption process; it showed that the plots do not go through the origin. Thus, a combination of intra-particle diffusion and film diffusion is believed to be the rate-limiting process for both adsorbents (Lalley *et al.* 2016).

Adsorption isotherms

Adsorption isotherm studies are important to determine the efficiency of adsorption. According to the linear form of the Langmuir isotherm (Equation (6)) and Freundlich isotherm (Equation (7)), Figure 3 shows the relationships between equilibrium FA concentration (C_e) and the equilibrium adsorption capacity (Q_e) at different temperatures (288 K, 298 K, 313 K). It was found that the adsorption of FA can be largely affected by temperature. The results showed that Q_e was inversely proportional to the operating temperature, which indicated that the adsorption of FA onto M-HPD 100 was an exothermic process. Figure 3(a) and 3(b) and Table 4 indicate that the Freundlich model gives a better fit than the Langmuir model. The high correlation coefficients ($R^2 =$ 0.9988) of the Freundlich model for all temperatures tested suggested that multi-layer adsorption occurred in FA removal with M-HPD 100. The value of n in the Freundlich model

Table 3 | Intra-particle diffusion parameters

Adsorbent	k_{p1} (mg g^{-1} min$^{-1/2}$)	C (mg/g)	R^2	k_{p2} (mg/g min$^{-1/2}$)	C (mg/g)	R^2
HPD 100	0.3084	−0.0245	0.9750	0.0552	0.9539	0.9541
M-HPD 100	0.4195	−0.0563	0.9894	0.0557	1.4067	0.9082

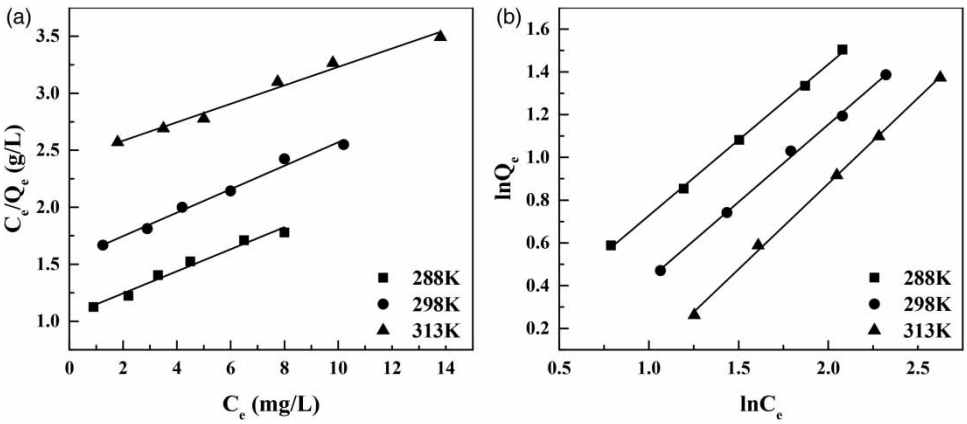

Figure 3 | The equilibrium isotherms for FA adsorbed by M-HPD 100 at different temperature (288 K, 298 K, 313 K): (a) the Langmuir model; (b) the Freundlich model. Pretreated macroporous resins of 2 g each, $C_0 = 5$ mg/L, 10 mg/L, 15 mg/L, 20 mg/L, 25 mg/L, 30 mg/L, $V_0 = 400$ mL, T = 288 K, 298 K, 313 K, pH = 7, 4 h of constant temperature water bath with oscillator speed 130 rpm.

Table 4 | Isotherm parameters for the adsorption of FA onto M-HPD 100

Isotherms	Parameters	Temperature (K)		
		288	298	313
Langmuir	q_m (mg/g)	9.97	10.28	12.80
	K_L	0.092	0.067	0.033
	R^2	0.9565	0.9675	0.9495
Freundlich	n	1.41	1.38	1.25
	K_f ($mg^{1-n}\ L^n\ g^{-1}$)	1.02	0.74	0.48
	R^2	0.9988	0.9973	0.9985

($n > 1$) showed a preferential adsorption; the present study speculates that the adsorption process seemed to involve physisorption.

The experimental data obtained at different temperatures were used in calculating the thermodynamic parameters such as Gibbs free energy change (ΔG), enthalpy change (ΔH) and entropy change (ΔS) (Equations (8) and (9)). Table 5 shows the thermodynamic parameters for the adsorption of FA onto M-HPD 100; $\Delta G < 0$ indicates that the adsorption process is spontaneous and irreversible; ΔS decrease with the increase of adsorption quantity means that when FA was dispersed in the surrounding solution and then adsorbed on the resin, the position was relatively fixed due to a series of physical or chemical actions, and the degree of freedom was reduced; thus the chaos of the whole adsorption system reduced and entropy decreased; $\Delta H < 0$ reveals that the adsorption of FA by resin is an exothermic process: with the increase of adsorption quantity, the surfaces of the highly active groups were gradually occupied, and the release of heat gradually reduced. When the adsorption of FA onto resin was within the range of 0.76–4.06 mg/g, ΔH was between −105 and −189 kJ/mol, which was higher than that of van der Waals force and hydrogen bonds. It indicates that the adsorption process of resin to FA includes not only physisorption but also chemisorption (which agrees with isotherm results and the Freundlich model, which assumed a multi-layer adsorption).

Table 5 | Thermodynamic parameters for the adsorption of FA onto M-HPD 100

Adsorption quantity q (mg/g)	ΔH	ΔG	ΔS
0.76	−189.1		0.57
1.52	−128.3		0.36
2.14	−120.7	−19.8	0.33
2.80	−116.1		0.32
3.39	−113.0		0.31
4.06	−105.0		0.29

Fixed-bed column test

To evaluate the practical application of M-HPD 100 for the continuous removal of FA from solution, fixed-bed column tests were conducted. Figures S7–S9 show the breakthrough curve for each adsorbent at different flow velocity, pH, and temperature respectively. As can be seen from Figure S7, the removal efficiency decreased with the increased flow velocity; the penetration time decreased and the dynamic adsorption capacity of the resin increased after modification. At 4 BV/h, the breakthrough points for M-HPD 100 occurred after about 14 h, and removal efficiency and dynamic adsorption quantity were 83.6% and

1.85 mg/L, respectively. Yet for HPD 100, breakthrough did not occur until about 16.7 h, and removal efficiency and dynamic adsorption quantity were 81.7% and 1.54 mg/L, respectively. Figures S8 and S9 indicate that M-HPD 100 was greatly affected by pH and temperature; the low-temperature and alkaline environment was conducive to the adsorption efficiency.

It is important to evaluate the above factors for the removal of FA by M-HPD 100, because the results indicate that the adsorbents' BET surface area does play an important role in breakthrough time of adsorption (Lalley *et al.* 2016). Also, it is postulated that the solution pH is another important parameter affecting the adsorption behavior (Hu *et al.* 2011). The effect of initial solution pH on FA removal by M-HPD 100 is shown in Figure S8. The adsorption of FA increased with pH increasing from 6.0 to 8.0. The results showed that at pH 6.0, 7.0, and 8.0, the maximum adsorption capacity of 1.09, 1.85, and 2.01 mg/g occurred at an initial FA concentration of 10 mg/L, respectively.

This is because the pH of the aqueous solution affects the speciation of FA and the surface charge of the adsorbent (Hu *et al.* 2011). On the one hand, under acidic conditions, FA exists in the form of gel in water, which agglomerates into spheres and increases the steric hindrance; on the other hand, low pH value (<7) is not conducive to the dissociation of carboxyl group, affecting the surface electrification of FA and the protonation of HPD 100 macroporous resin grafted with amino groups. In an alkaline environment (pH <8.3), FA particles extend, acidic functional groups dissociate, and it is easy for FA to interact with the surface of the proton resin; FA itself is more likely to form a negatively charged hydrophilic colloid, which results in a stronger attraction for a protonated cationic form ($-NH_3^+$) in the solution, and electrostatic interaction occurs between the adsorbent and $-COO^-$ ions (primary) resulting in high FA removal with low steric resistance, which makes it more likely for FA to enter into the resin pores and physical adsorption to take place.

Thermodynamic consideration of an adsorption process is necessary to conclude whether the process is spontaneous or not. Consistent with what we discussed above, the adsorption of FA decreased with T increasing from 288 K to 313 K. The results indicated that at 288 K, 298 K, and 313 K, the maximum adsorption capacity of 1.99, 1.85, and 1.23 mg/g occurred at an initial FA concentration of 10 mg/L, respectively. The results showed that M-HPD 100 still has properties of physical adsorption, which is an exothermic process, conforming with physical adsorption law.

Desorption studies

The regenerated M-HPD 100 was reused for six adsorption–desorption cycles and the results are illustrated in Figure 4. Desorption was carried out with NaOH. It was observed that 64.28% of the loaded FA was stripped in 50% NaOH in the sixth cycle, and 74% adsorption efficiency occurred after six cycles of regeneration, perhaps due to the dual competition of both the anions ($-COO^-$ and OH^-) to be adsorbed on the surface of the adsorbent, of which OH^- predominates, promoting desorption. The apparent poor recovery observed in basic media NaOH, may be due to the adsorbent's surface being deprotonated; hence detachment of the bound anions from the copolymer is difficult. Complete desorption is not possible (Singh *et al.* 2007), perhaps due to the involvement of non-electrostatic forces between the M-HPD 100, and the further desorption of FA is hindered by the porosity of the adsorbent.

Adsorption of FA from natural water

The copolymer was also evaluated for the FA removal from a natural water sample containing FA using 2 g adsorbent. From Figure 5, the breakthrough points for HPD 100 and M-HPD 100 occurred after about 6.65 h and 9.2 h, respectively; removal efficiency and dynamic adsorption quantity were 45.2% and 54.3% and 0.85 mg/L and 0.64 mg/L, respectively. It can be seen from Figure 6 that the removal rate of FA by the modified resin reached 71.1%. When the desorption experiment was conducted for 140 min, the FA concentration reached the maximum value; when the desorption experiment was conducted for 320 min, the FA concentration reached stability and the desorption rate

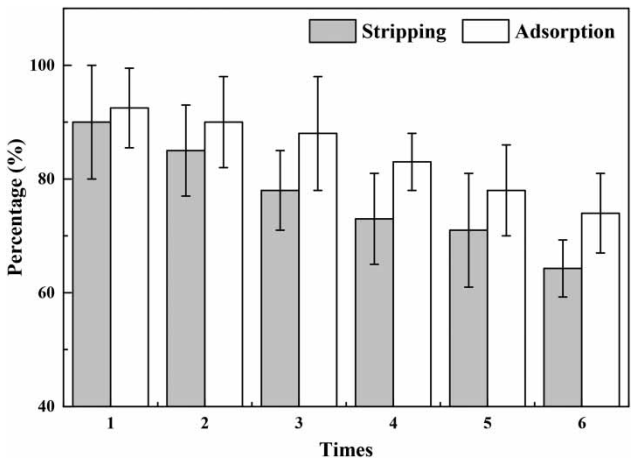

Figure 4 | Adsorption and desorption efficiency after multiple regeneration.

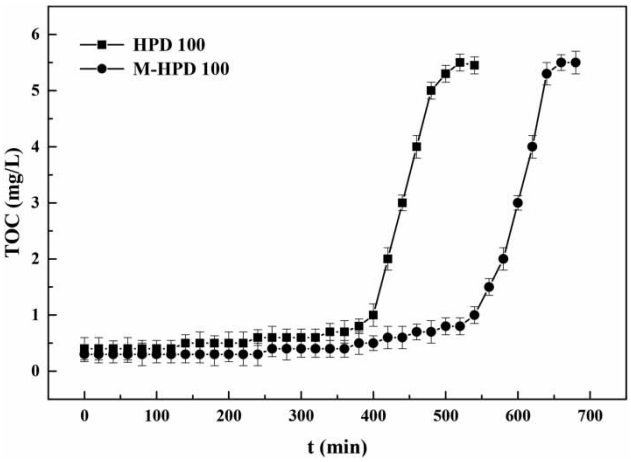

Figure 5 | The dynamic adsorption curve of two kinds of resins to the water of Mopanshan Reservoir. Pretreated macroporous resins of 2 g each, TOC = 5.5 mg/L, chemical oxygen demand = 3.53 mg/L, T = 286 K, pH = 7.5, v = 4 BV/h.

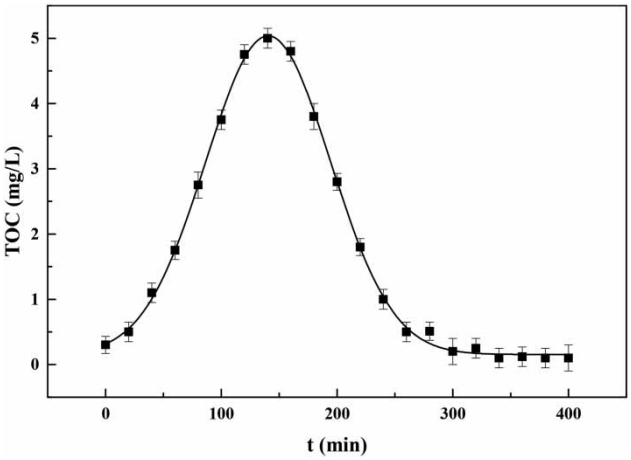

Figure 6 | Dynamic desorption curve of Mopanshan Reservoir water. Pretreated macroporous resins of 2 g each, pH = 7, T = 313 K, v = 2 BV/h.

was 76.1%. It was observed that the adsorbent was more efficient in adsorbing from laboratory solutions. In natural water the adsorbent capacity was low, which may be due to the presence of other substances in water which interfere with the FA adsorption. However, the product was found useful in treating natural water contaminated with specific molecular sizes of FA.

CONCLUSIONS

The present study focuses on adsorption of FA from aqueous solution using the M-HPD 100 as an effective adsorbent. Adsorption of FA is found to be effective at higher pH and at lower temperatures. In addition, the very fast adsorption for the M-HPD 100 makes this material suitable for continuous flow water treatment systems. Equilibrium isotherm data were fitted using different two-parameter models. Among these models, the Freundlich model was in good agreement with the experimental data with high R^2 (0.9988). The kinetic study showed that the pseudo-second-order model was appropriate to describe the experiment results. Intra-particle diffusion and film diffusion were believed to be the rate-limiting processes. The dependence of adsorption of FA on temperature, pH and flow velocity was investigated and the thermodynamic parameters ΔG, ΔH and ΔS were calculated. The results show a feasible, spontaneous and exothermic multi-layer physicochemical adsorption process. The adsorption–desorption cycle results demonstrated that the regeneration and subsequent use of the M-HPD 100 would enhance the economics of practical applications for the removal of FA from actual water samples.

ACKNOWLEDGEMENTS

The research was financially supported by Open Project of State Key Laboratory of Urban Water Resource and Environment, Harbin Institute of Technology with the grant no. HCK201804. And we also greatly thank the reviewers for their insightful and valuable suggestions.

SUPPLEMENTARY MATERIAL

The Supplementary Material for this paper is available online at https://dx.doi.org/10.2166/wst.2020.187.

REFERENCES

Aeschbacher, M., Graf, C., Schwarzenbach, R. P. & Sander, M. 2012 Antioxidant properties of humic substances. *Environmental Science & Technology* **46** (9), 4916–4925. doi:10.1021/es300039 h.

Ang, W. L., Mohammad, A. W., Hilal, N. & Leo, C. P. 2015 A review on the applicability of integrated/hybrid membrane processes in water treatment and desalination plants. *Desalination* **363**, 2–18. doi:10.1016/j.desal.2014.03.008.

Bhatnagar, A. & Sillanpaa, M. 2017 Removal of natural organic matter (NOM) and its constituents from water by adsorption – a review. *Chemosphere* **166**, 497–510. doi:10.1016/j.chemosphere.2016.09.098.

Bolto, B., Dixon, D., Eldridge, R., King, S. & Linge, K. 2002 Removal of natural organic matter by ion exchange. *Water Research* **36** (20), 5057–5065. https://doi.org/10.1016/S0043-1354(02)00231-2.

Cabaniss, S. E., Zhou, Q., Maurice, P. A., Chin, Y. & Aiken, G. R. 2000 A log-normal distribution model for the molecular weight of aquatic fulvic acids. *Environmental Science & Technology* **34** (6), 1103–1109. doi:10.1021/es990555y.

Cheng, M., Zeng, G., Huang, D., Lai, C., Liu, Y., Zhang, C., Wang, R., Qin, L., Xue, W., Song, B., Ye, S. & Yi, H. 2018 High adsorption of methylene blue by salicylic acid–methanol modified steel converter slag and evaluation of its mechanism. *Journal of Colloid and Interface Science* **515**, 232–239. doi:10.1016/j.jcis.2018.01.008.

Cheung, W. H., Szeto, Y. S. & McKay, G. 2007 Intraparticle diffusion processes during acid dye adsorption onto chitosan. *Bioresource Technology* **98** (15), 2897–2904. doi:10.1016/j.biortech.2006.09.045.

Deng, L., Ye, L., Hou, S., Chen, G. & Chen, C. 2004 Study on quality evaluation methods of pretreatment for polystyrene-type macroporous absorbing resins. *Zhongguo Zhong yao za zhi=Zhongguo zhongyao zazhi=China Journal of Chinese Materia Medica* **29** (11), 1037–1040.

Eris, S. & Bashiri, H. 2016 Kinetic study of the adsorption of dyes onto activated carbon. *Progress in Reaction Kinetics and Mechanism* **41** (2), 109–119. doi:10.3184/146867816X14570175656394.

Fan, T., Liu, Y., Feng, B., Zeng, G., Yang, C., Zhou, M., Zhou, H., Tan, Z. & Wang, X. 2008 Biosorption of cadmium(II), zinc(II) and lead(II) by *Penicillium simplicissimum*: isotherms, kinetics and thermodynamics. *Journal of Hazardous Materials* **160** (2–3), 655–661. doi:10.1016/j.jhazmat.2008.03.038.

Ghaedi, M., Ghaedi, A. M., Negintaji, E., Ansari, A., Vafaei, A. & Rajabi, M. 2014 Random forest model for removal of bromophenol blue using activated carbon obtained from *Astragalus bisulcatus* tree. *Journal of Industrial and Engineering Chemistry* **20** (4), 1793–1803. https://doi.org/10.1016/j.jiec.2013.08.033.

Hasan, Z. & Jhung, S. H. 2015 Removal of hazardous organics from water using metal-organic frameworks (MOFs): plausible mechanisms for selective adsorptions. *Journal of Hazardous Materials* **283**, 329–339. doi:10.1016/j.jhazmat.2014.09.046.

Ho, Y. S. & McKay, G. 1998 Kinetic models for the sorption of dye from aqueous solution by wood. *Process Safety and Environmental Protection* **76** (2), 183–191. doi:10.1205/095758298529326.

Hu, X., Wang, J., Liu, Y., Li, X., Zeng, G., Bao, Z., Zeng, X., Chen, A. & Long, F. 2011 Adsorption of chromium (VI) by ethylenediamine-modified cross-linked magnetic chitosan resin: isotherms, kinetics and thermodynamics. *Journal of Hazardous Materials* **185** (1), 306–314. doi:10.1016/j.jhazmat.2010.09.034.

Jiang, Z., Li, A., Cai, J., Wang, C. & Zhang, Q. 2007 Adsorption of phenolic compounds from aqueous solutions by aminated hypercrosslinked polymers. *Journal of Environmental Sciences* **2** (19), 135–140. doi:10.1016/s1001-0742(07)60022-9.

Lalley, J., Han, C., Li, X., Dionysiou, D. D. & Nadagouda, M. N. 2016 Phosphate adsorption using modified iron oxide-based sorbents in lake water: kinetics, equilibrium, and column tests. *Chemical Engineering Journal* **284**, 1386–1396. doi:10.1016/j.cej.2015.08.114.

Lin, M., Zhao, Z., Cui, F. & Xia, S. 2012 Modeling of equilibrium and kinetics of chlorobenzene (CB) adsorption onto powdered activated carbon (PAC) for drinking water treatment. *Desalination And Water Treatment* **1–3** (44), 245–254. doi:10.1080/19443994.2012.691746.

Liu, F., Chen, J., Li, A., Fei, Z., Zhu, Z. & Zhang, Q. 2003 Properties and thermodynamics of adsorption of benzoic acid onto XAD-4 and a water-compatible hypercrosslinked adsorbent. *Chinese Journal of Polymer Science* **21** (3), 317–324.

Matilainen, A. & Sillanpää, M. 2010 Removal of natural organic matter from drinking water by advanced oxidation processes. *Chemosphere* **80** (4), 351–365. doi:10.1016/j.chemosphere.2010.04.067.

Matyjaszewski, K. 2012 Atom transfer radical polymerization (ATRP): current status and future perspectives. *Macromolecules* **45** (10), 4015–4039. doi:10.1021/ma3001719.

Sillanpää, M., Ncibi, M. C., Matilainen, A. & Vepsäläinen, M. 2018 Removal of natural organic matter in drinking water treatment by coagulation: a comprehensive review. *Chemosphere* **190**, 54–71. doi:10.1016/j.chemosphere.2017.09.113.

Singh, V., Tiwari, S., Sharma, A. K. & Sanghi, R. 2007 Removal of lead from aqueous solutions using *Cassia grandis* seed gum-graft-poly(methylmethacrylate). *Journal of Colloid and Interface Science* **316** (2), 224–232. doi:10.1016/j.jcis.2007.07.061.

Sophia, A.,C. & Lima, E. C. 2018 Removal of emerging contaminants from the environment by adsorption. *Ecotoxicology and Environmental Safety* **150**, 1–17. doi:10.1016/j.ecoenv.2017.12.026.

Tan, L. & Tan, B. 2017 Hypercrosslinked porous polymer materials: design, synthesis, and applications (vol. 42, pg 3322, 2017). *Chemical Society Reviews* **46** (11), 3481. doi:10.1039/c7cs90027a.

Tang, F., Zhang, L., Zhang, Z., Cheng, Z. & Zhu, X. 2009 Cellulose filter paper with antibacterial activity from surface-initiated ATRP. *Journal of Macromolecular Science, Part A* **46** (10), 989–996. doi:10.1080/10601320903158651.

Wang, H., Liu, R., Liu, Y., Meng, Y., Liu, Y., Zhai, H. & Di, D. 2019 Investigation on adsorption mechanism of peptides with surface-modified super-macroporous resins. *Langmuir* **35** (13), 4471–4480. doi:10.1021/acs.langmuir.8b03997.

Wu, X., Jiang, W., Luo, Y. & Li, J. 2019 Poly(aspartic acid) surface modification of macroporous poly(glycidyl methacrylate) microspheres. *Journal of Applied Polymer Science* **47441**. doi:10.1002/app.47441.

Xiao, G., Wen, R., Wei, D. & Wu, D. 2016 A novel hyper-cross-linked polymeric adsorbent with high microporous surface area and its adsorption to theophylline from aqueous

solution. *Microporous and Mesoporous Materials* **228**, 168–173. doi:10.1016/j.micromeso.2016.03.048.

Zhang, P. & Wang, L. 2010 Extended Langmuir equation for correlating multilayer adsorption equilibrium data. *Separation and Purification Technology* **70** (3), 367–371. doi:10.1016/j.seppur.2009.10.007.

Zhang, W., Du, Q., Pan, B., Lv, L., Hong, C., Jiang, Z. & Kong, D. 2009 Adsorption equilibrium and heat of phenol onto aminated polymeric resins from aqueous solution. *Colloids and Surfaces A: Physicochemical and Engineering Aspects* **346** (1–3), 34–38. doi:10.1016/j.colsurfa.2009.05.022.

Zheng, Y. J. 2011 吸附树脂接枝聚合物刷及其对氯仿吸附性能的研究 *(Study on Adsorption Properties of Chloroform with Resin Grafted with Polymer Brush)*. PhD thesis, Harbin Institute of Technology, Harbin, China, Chinese.

Zhu, L., Deng, Y., Zhang, J. & Chen, J. 2011 Adsorption of phenol from water by N-butylimidazolium functionalized strongly basic anion exchange resin. *Journal of Colloid and Interface Science* **364** (2), 462–468. doi:10.1016/j.jcis.2011.08.068.

First received 5 July 2019; accepted in revised form 6 April 2020. Available online 22 April 2020